

Article - Engineering, Technology and Techniques

Computational Buckling Analysis of Epoxy-Based Composite Reinforced with Sugarcane Fiber, Fly-Ash, and Carbon Nanotube

Sai Srikar Lanka¹

<https://orcid.org/0009-0001-7556-5511>

Krishanu Borah¹

<https://orcid.org/0009-0009-9255-7386>

Venkatachalam Gopalan^{2*}

<https://orcid.org/0000-0002-5051-139X>

Vignesh Prakasam³

<https://orcid.org/0000-0002-9364-9970>

Giriraj Mannayee⁴

<https://orcid.org/0000-0002-8726-2972>

¹Vellore Institute of Technology, School of Mechanical Engineering, Chennai, Tamilnadu, India; ²Vellore Institute of Technology, Centre for Innovation and Product Development, Chennai, Tamilnadu, India; ³EinNel Technologies, CAE Automotive, Chennai, Tamilnadu, India; ⁴Vellore Institute of Technology, School of Mechanical Engineering, Vellore, Tamilnadu, India.

Editor-in-Chief: Alexandre Rasi Aoki
Associate Editor: Alexandre Rasi Aoki

Received: 22-Apr-2022; Accepted: 14-Feb-2023

*Correspondence: g.venkatachalam@vit.ac.in; Tel.: +91-73582 44532 (V.G.)

HIGHLIGHTS

- An attempt to reuse industrial waste for new product development.
- Sugarcane, an agricultural waste and fly-ash, an industrial waste were used.
- Buckling analysis were simulated for epoxy polymer.
- Design of Experiment and optimization were used in the research.

Abstract: Industries play a very vital role in the developed nation. Proportional to the higher production capacity of these industries, there is a surge in the quantity of waste material being discharged. This waste material can be put to effective use; a considerable way is by creating a green composite that is long-lasting, and concocted by using natural fibers and environment-friendly materials as reinforcements. In the following study, an attempt is made to investigate the buckling characteristics of a thin geometrical plate of epoxy-based composite reinforced with Sugarcane fiber/ Fly-ash/ Carbon Nanotube. The investigative study was conducted numerically on the plate by applying axially compressive load. To procure an optimized result on the weight percentages of the composition of the fiber in the composite material, the DOE/optimization tool i.e. a mathematical and statistical technique known as the Response Surface Methodology (RSM) was used. Essential geometrical modeling and the appropriate boundary conditions for the buckling analysis were

carried out using the Static Structural and Eigen Buckling standalone systems in the ANSYS software. The analytical tool, Analysis of Variance (ANOVA) was utilized to investigate the influential degree of reinforcement variables on buckling characteristics present in the composite. The results reveal that the critical buckling loads escalate for higher weight percentages for carbon nanotube and fly-ash reinforcements in the composite composition. The optimized parameters obtained can be incorporated to achieve improved critical buckling load and hence many synthetic composites were replaced thus enhancing the sustainability of the environment.

Keywords: Polymer composite; Sugarcane fiber; Carbon Nanotube; Response Surface Methodology; Analysis of Variance; Critical Buckling Load.

INTRODUCTION

The development of a country is heavily reliant on the industries present in that particular nation. As a nation would start climbing up the ladder of progress in search of higher development, the production demands from the industries present in the country would massively surge. This significant spike in the production demands across various industries in the nation tends to increase the production supply and capacity of the industries. On the other hand, the amount of waste material discharged from these industries is also bound to increase since the amount of waste material discharged is in direct proportion to their increased production capacity. An environment-friendly constructive solution to this problem would be to fabricate a sustainable green composite that is made out of natural fibers and biodegradable materials as a replacement for the conventional synthetic fibers being used as reinforcements.

Rhodes [1] presented an analysis of compressed plate behavior in which the effects of buckling deflections on the plate membrane strains and stresses were discussed based on geometrical analysis. May-Pat and coauthors [2] mentioned that natural fibers, being environmentally friendly, have good properties compared to synthetic ones. Philippou and Karastergiou [3] concluded that due to increasing concerns about the environment and the ecosystem, research in developing natural fiber-based composites saw a sudden spark. Besides, it was proven that composites demonstrate better properties than the constituent materials may not exhibit [4-7]. Matuana and Stark [8] studied the effects of adding wood fibers as reinforcements in composites and concluded that wood polymer composites with a low melt flow index show better tensile and impact properties. Kumar and coauthors [9] presented that sugar fibers show better flexural strength and impact strength. Thermosets polymer is strongly cross-linked polymers that are cured using heat, pressure, and light irradiation, resulting in a structure that is highly flexible for setting forth desired final qualities as well as improved strength and modulus [10-14].

Traditionally, bagasse has been used majorly as a fuel for boilers in sugar factories and a small portion is used for making paper and board [15-16]. But the low calorific value makes them a poor fuel for energy generation and hence their application in the boiler industry would thus decline in the future [16-18]. The addition of natural fibers along with chopped glass fibers resulted in the enhancement of the mechanical properties of the composite. Gopalan and coauthors [19] examined the effects of flax/epoxy laminated composite plates under axial compressive load. They concluded that the number of layers, width, and orientation of the composite influence the load-carrying capacity and elastic moduli of the composite.

Apart from these biological reinforcements, fly ash is another substance that is massively produced as a by-product of coal-fired power stations. Singla and Chawla [20] concluded that the compressive strength of an epoxy resin and fly ash composite can be enhanced with the inclusion of fly ash particles due to the strong interfacial relationship between fly ash and resin and the hollowness of fly ash particles. Sim and coauthors [21] investigated the effects of adding fly ash to epoxy resin on its mechanical properties. It was observed that the tensile strength of the composite tends to rise as the volume fraction of fly ash that is added to the composite is also increased up to a certain threshold limit, after which on further addition of the fly ash the tensile strength of the composite begins to decline.

In contemporary days, to attain the fitting mechanical properties, composites are being fabricated by using Carbon Nanotubes (CNT) as a filler/reinforcement. Harris [22] assessed that the best mechanical properties of a CNT reinforced composite are found with arc-grown nanotubes, with well-dispersed tubes throughout the matrix. Another important point is to achieve good bonding between nanotubes and matrix as can be seen from the work of Gojny and coauthors [23]. They stated that the dispersion of the nanotubes in an epoxy system can be improved by the chemical functionalization of the multi-walled carbon nanotubes. Moreover, carbon nanotubes are really good electrical conductors having current densities of up to 10 Am⁻² and great thermal conductivities [24-28]. Many of these excellent properties can be best exploited by integrating these nanotubes in some kind of matrix, which has been a rapidly growing field of study [29-30].

From the literature review, it is noted that not much work has been reported in the field of buckling analysis of sugarcane fiber, fly ash, and carbon nanotube (CNT) laminated epoxy polymer matrix composite. Here, the authors attempt to study the buckling characteristics of sugarcane / fly ash / CNT-reinforced epoxy polymer composite.

MATERIAL AND METHODS

The critical buckling load plays a very crucial role in determining whether a structure buckles or not when subjected to axial compressive loading. To obtain the critical buckling load, a few parametric inputs must first be known which is dependent on the plate dimensions. The aspect ratio 'r' of the geometric model is used to extrapolate the curves in the plot by the boundary conditions of the geometry to the buckling coefficient 'k'; an important parameter to calculate the critical buckling load.

The final critical buckling load is derived from the plate bending stiffness 'D' which in turn is related to the properties of the material. The bending stiffness of the plate can be formulated as mentioned in equation 1.

$$D = E h^3 / 12(1 - \nu^2) \quad (1)$$

In the above equation, the constants of the geometry include the thickness 'h' and the material properties include, Young's modulus 'E' and Poisson's ratio 'ν'.

The obtained bending stiffness value is then substituted in equation 2, to procure the final critical buckling load.

$$N_{xcr} = k \pi^2 D / b^2 \quad (2)$$

Where 'N_{xcr}' is the critical buckling load, 'b' is the breadth of the plate and 'k' is the buckling coefficient which is obtained by extrapolation of the curve intercepting the boundary condition of the model and the aspect ratio.

The buckling coefficient of the model, used in equation 2, needs to be interpolated from Figure 1 which is based on buckling coefficients resulting due to the corresponding boundary conditions acting on rectangular plates.

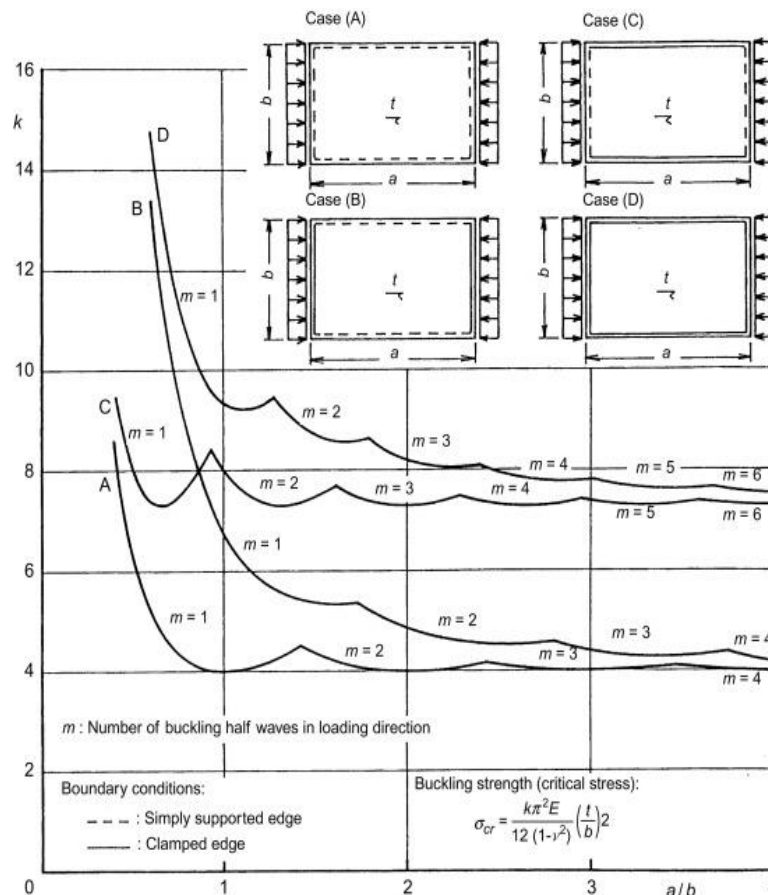


Figure 1. Buckling coefficients of rectangular plates according to respective in-plane boundary conditions [31]

Geometrical model and design of experiments

A thin plate of 3m length and 1m breadth is designed using the Design Modeler of ANSYS18. The thickness of the plate is 2mm. The geometry is modeled and meshed using the 'BRICK 8 node 185' element with an element size of 5 mm. The finite element model has 7301 nodes and 7588 elements. Simply supported boundary conditions are provided to the meshed geometry where the top and bottom edges are constrained along with U_z and Rot_Y . Similarly, the left and right edges are constrained along with U_z and Rot_X . A compressive load of 10N is provided along the top and bottom edges after selecting all the nodes present along these edges. Figure 2(a) depicts the meshed model, Figure 2(b) shows the boundary conditions applied to the finite element model, and Figure 2(c) shows the loading conditions applied to the finite element model.

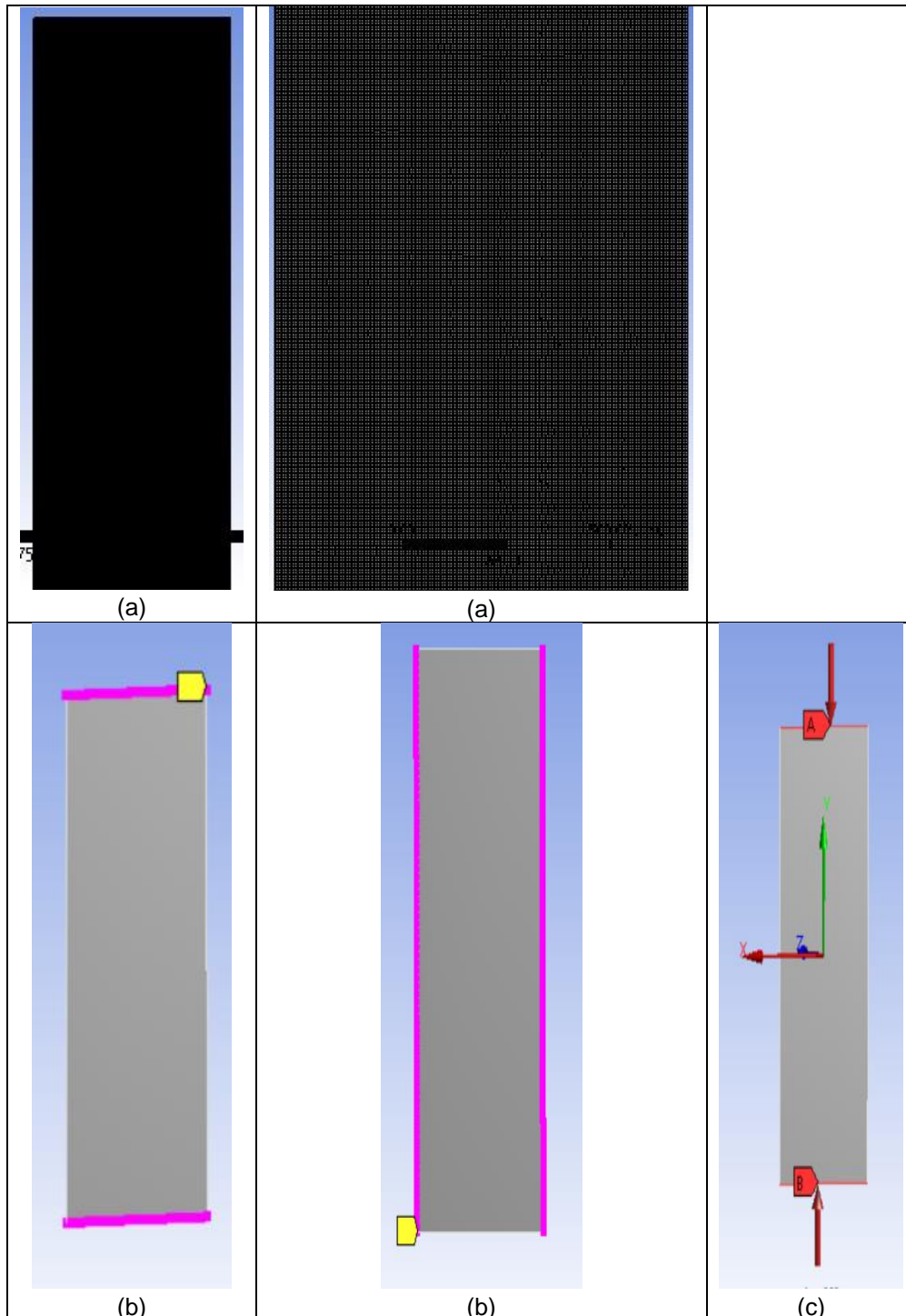


Figure 2. Epoxy composite plate: (a) Meshed plate; (b) plate with simply supported boundary conditions; (c) the axial compressive load of 10N.

A Central Composite Design (CCD), which is one of the designs under the Response Surface Methodology is created. RSM is employed in this study as it performs the role of optimization along with playing the Design of Experiments (DOE) role. For the following study, 5 distinct levels for each weight percentage of the Sugarcane fiber, Fly-ash fiber, and Carbon Nanotube are taken into account. The values of wt. % for the sugarcane and fly-ash fibers are varied between the extent of 0 and 2. Similarly, the values of wt. % corresponding to MWCNT are constrained in the domain between 0 and 1. The coded values and their corresponding weight percentage values for each of the respective fibers are tabulated and presented in Table 1.

Table 1. Weight percentage levels of sugarcane fiber, fly-ash fiber, and CNT with their respective coded values.

Parameters	Levels				
	-2	-1	0	1	2
Wt. % of Sugarcane fiber	0	0.5	1.0	1.5	2.0
Wt. % of CNT	0	0.25	0.5	0.75	1.0
Wt. % of Fly-ash fiber	0	0.5	1.0	1.5	2.0

There were 20 different combinations with variations in the wt. % of sugarcane fiber / fly ash / MWCNT are obtained by creating CCD / RSM using the Minitab software. The samples with varied wt. % of fibers are simulated using their respective material properties using ANSYS18 software. Table 2 represents the different samples with their respective coded values.

Table 2. Samples obtained from CCD with actually varied wt. % of fibers and their corresponding coded values.

Sample Number	Wt.% of sugarcane		Wt.% of CNT		Wt.% of Fly-ash	
	Actual	Coded	Actual	Coded	Actual	Coded
1	0.5	-1	0.75	1	0.5	-1
2	1	0	0.5	0	1	0
3	1.5	1	0.25	-1	0.5	-1
4	1	0	0.5	0	1	0
5	1.5	1	0.75	1	1.5	1
6	0.5	-1	0.25	-1	1.5	1
7	1	0	0.5	0	1	0
8	1	0	0.5	0	2	2
9	0	-2	0.5	0	1	0
10	1	0	0.5	0	0	-2
11	1	0	1	2	1	0
12	1	0	0	-2	1	0
13	2	2	0.5	0	1	0
14	1	0	0.5	0	1	0
15	1	0	0.5	0	1	0
16	1	0	0.5	0	1	0
17	1.5	1	0.25	-1	1.5	1
18	0.5	-1	0.75	1	1.5	1
19	0.5	-1	0.25	-1	0.5	-1
20	1.5	1	0.75	1	0.5	-1

RESULTS and DISCUSSION

Critical Buckling Loads

Table 3 represents the results of simulations which is carried out based on the varied wt. % of reinforcements according to the values in Table 2. Simulations, for each combination present in Table 2, are carried out using the Eigen Value Buckling standalone system available in ANSYS18 software and are tabulated in Table 3.

Table 3. Critical buckling loads obtained after performing Eigen Value Buckling simulations for different combinations

Sample Number	Wt.% of sugarcane		Wt.% of CNT		Wt.% of Fly-ash		Critical Buckling load (N) Through ANSYS	Critical Buckling load (N) through Empirical Formula
	Actual	Coded	Actual	Coded	Actual	Coded		
1	0.5	-1	0.75	1	0.5	-1	51.75	51.67
2	1	0	0.5	0	1	0	51.13	61.12
3	1.5	1	0.25	-1	0.5	-1	37.39	37.32
4	1	0	0.5	0	1	0	51.13	61.12
5	1.5	1	0.75	1	1.5	1	52.72	52.65
6	0.5	-1	0.25	-1	1.5	1	38.34	38.27
7	1	0	0.5	0	1	0	51.13	61.12
8	1	0	0.5	0	2	2	47.27	47.19
9	0	-2	0.5	0	1	0	69.39	69.26
10	1	0	0.5	0	0	-2	61.12	61.02
11	1	0	1	2	1	0	52.19	52.10
12	1	0	0	-2	1	0	42.18	42.11
13	2	2	0.5	0	1	0	54.27	54.18
14	1	0	0.5	0	1	0	51.13	61.12
15	1	0	0.5	0	1	0	51.13	61.12
16	1	0	0.5	0	1	0	51.13	61.12
17	1.5	1	0.25	-1	1.5	1	47.74	47.65
18	0.5	-1	0.75	1	1.5	1	66.88	66.75
19	0.5	-1	0.25	-1	0.5	-1	54.38	54.27
20	1.5	1	0.75	1	0.5	-1	53.43	53.32

Figure 3 and Figure 4 represent the Eigen Value Buckling simulation results which are obtained based on the half-wave theory [11] dealing with the buckling of thin plates.

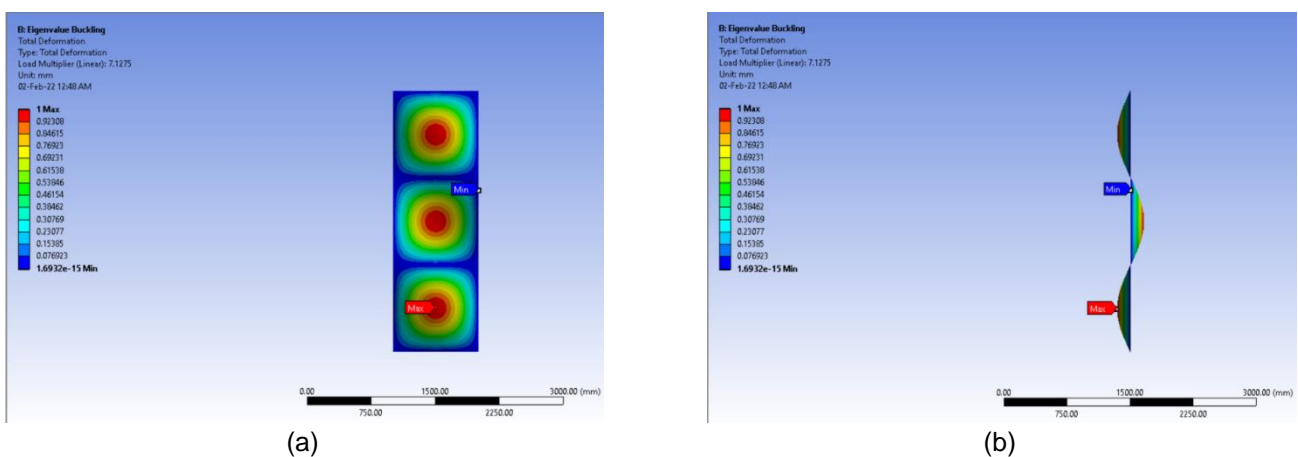


Figure 3. Eigen Value Buckling simulation result depicting half-waves obtained: (a) Front view; (b) Side view.

For the samples presented in Table 3, the critical buckling loads obtained after ANSYS simulations are compared to the resultant critical buckling loads procured by using the empirical formula based on the buckling plate theory. As in the case depicted in Figure 3 and for the first sample in Table 3, the corresponding critical buckling load obtained by ANSYS simulation is 51.754 N. The critical buckling load is calculated for the aforementioned sample using the empirical formula, i.e. about equations 2 and 3, for which the resultant value obtained is 51.67 N. On carrying out an error percentage evaluation, the error obtained between the theoretical result and the ANSYS simulation result is found to be a marginal error of 0.16%. Similarly, by the results obtained by ANSYS simulations and empirical formula, error percentages are calculated for a few more samples as presented in Table 4.

Table 4. Comparison between critical buckling loads obtained by empirical formula and ANSYS Eigen Value Buckling simulations

Sample Number	Critical Buckling Load obtained by Empirical formula	Critical Buckling Load obtained by ANSYS simulation	Error %
1	51.67	51.75	0.16
2	61.12	51.13	16.34
3	37.32	37.39	0.17
4	61.12	51.13	16.34
5	52.65	52.72	0.13
6	38.27	38.34	0.16
7	61.12	51.13	16.34
8	47.19	47.26	0.15
9	69.26	69.39	0.18
10	61.02	61.12	0.16
11	52.10	52.19	0.15
12	42.11	42.18	0.16
13	54.18	54.27	0.15
14	61.12	51.13	16.34
15	61.12	51.13	16.34
16	61.12	51.13	16.34
17	47.65	47.74	0.18
18	66.75	66.87	0.18
19	54.27	54.38	0.20
20	53.32	53.43	0.20

Regression Equation

Minitab software is used for statistical analysis of the results which are obtained using ANSYS18 by performing simulations varying the wt. % of Sugarcane fiber/ fly ash / MWCNT. The statistical analysis leads to a regression equation and the same is validated with ANSYS simulation results. The procured equations are used to signify the aspect by which the varied weight percentages of sugarcane fiber/ fly ash and MWCNT would be impacting the buckling behavior of the thin composite plate. From the regression equation, presented in equation 3, critical buckling loads are obtained for all the 20 sample combinations mentioned in Table 2. Tabulation of the critical buckling loads derived from the regression equation, along with the error percentages calculated based on the values obtained from the computational simulation using ANSYS and regression equation is presented in Table 5.

$$\text{Critical buckling load} = 80.2 - 34.6A + 0.4B - 27.6C + 10.91A^2 - 9.4B^2 + 3.28C^2 + 1.1AB + 5.88BC + 26.1 AC \quad (3)$$

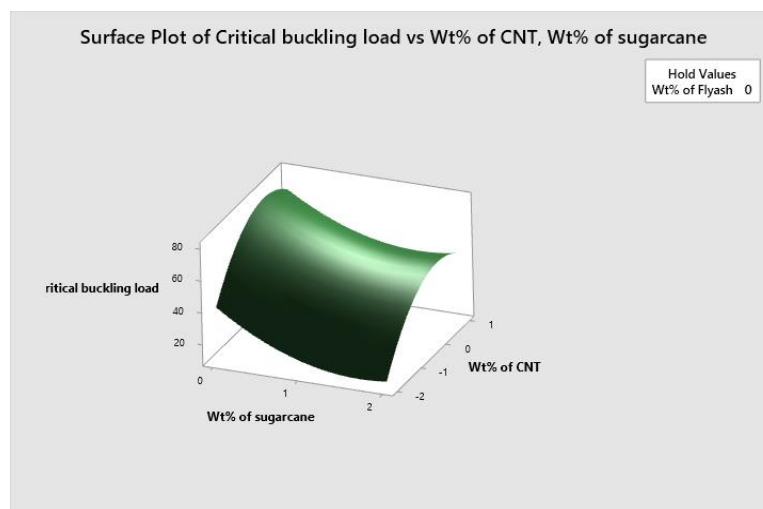
Where A – wt. % of sugarcane; B – wt. % of CNT; C – wt. % of fly ash

Table 5. Error percentage between regression equation results and ANSYS18 Eigen Value Buckling simulation results

Sample number	ANSYS	Regression	Error %
1	51.75	59.18	12.55
2	51.13	49.22	3.87
3	37.39	47.31	20.96
4	51.13	49.22	3.87
5	52.72	57.22	7.86
6	38.34	45.00	14.81
7	51.13	49.22	3.87
8	47.26	50.09	5.64
9	69.39	66.48	4.37
10	61.12	54.91	11.30
11	52.19	55.98	6.77
12	42.18	37.77	11.67
13	54.27	53.78	0.91
14	51.13	49.22	3.87
15	51.13	49.22	3.87
16	51.13	49.22	3.87
17	47.74	41.32	15.55
18	66.87	60.36	10.79
19	54.38	56.88	4.38
20	53.43	50.17	6.51

Surface Plot

Figure 4 illustrates a surface plot of the influence of sugarcane fiber weight percent and CNT weight percent on the composite's critical buckling load, with the effect of the fly-ash set to 0. According to the plot obtained, the maximum critical buckling load is achieved at 1.5% of sugarcane fiber and 0.75% of CNT [32]. Meanwhile, the minimum critical buckling load for the same plot is 2% of sugarcane fiber and 0% of CNT fiber. Likewise, Figure 5 shows a surface plot of the effect of fly-ash weight percent and CNT weight percent on the critical buckling load of the composite when the influence of sugarcane fiber is constrained to 0. On close observation of this plot, it can be noted that the maximum critical buckling load is achieved at weight percentages of 2% fly ash and 0.75% CNT. On the contrary, a minimum buckling load is observed in the surface plot for 0.25 wt. % of CNT and 2 wt.% of fly-ash combination. Figure 6 illustrates a surface plot in which the weight percentages of fly-ash fiber and sugarcane fibers are presented, while the wt. % of CNT is set to 0. The plot shows that the maximum critical buckling load is achieved at weight percentages of 1.5% fly ash fiber and 2% of sugarcane fiber. On the other hand, the minimum critical buckling load is observed at weightage percentages of 1% sugarcane fiber and 2% fly-ash fiber.

**Figure 4.** Critical Buckling Load versus Wt.% of CNT and sugarcane fibers

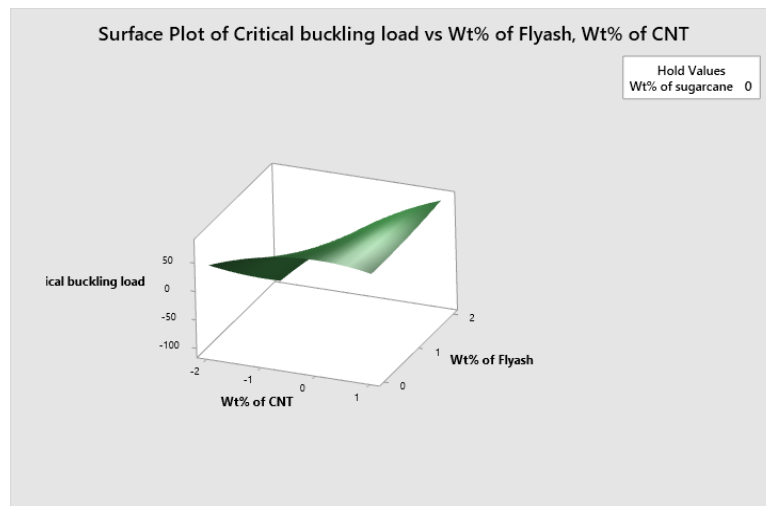


Figure 5. Critical Buckling Load versus Wt.% of fly-ash fiber and CNT

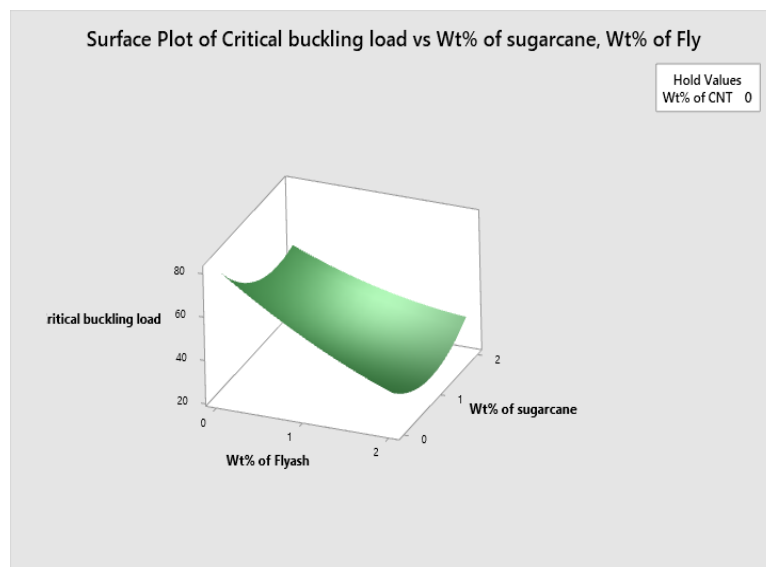


Figure 6. Critical Buckling Load versus Wt.% of sugarcane and fly-ash fibers

Parametric Optimization to achieve Maximum Critical Buckling Load

Using the RSM optimization tool available in Minitab, an optimized parametric evaluation is run and an optimized result has a maximum critical buckling load for a suitable combination of wt. % of reinforcements in the composite are procured. The optimized results are tabulated as shown in Table 6. According to the table, the combination produces a maximum critical buckling load which is at 80.80 N for a wt. % of sugarcane fiber at 2%, wt. % of CNT at 0.75% and wt. % of fly-ash fly ash. The optimum results are validated using the ANSYS18 software by simulating the same geometrical model by giving the material property inputs corresponding to the combination offering the maximum critical buckling load and the result were shown in Figure 7. The simulation result for the optimized parametric combination is not aberrant from the optimized result obtained using the RSM optimizer and finally, the error percentage is calculated at 8.67%.

Table 6. Optimized parameters representing the combination for achieving maximum critical buckling load

wt. % of sugarcane fiber	wt. % of CNT	wt. % of fly-ash	Maximum critical buckling load (RSM optimizer)	Maximum critical buckling load (ANSYS18)	Error %
2	0.75	2	80.80 N	73.82 N	8.67

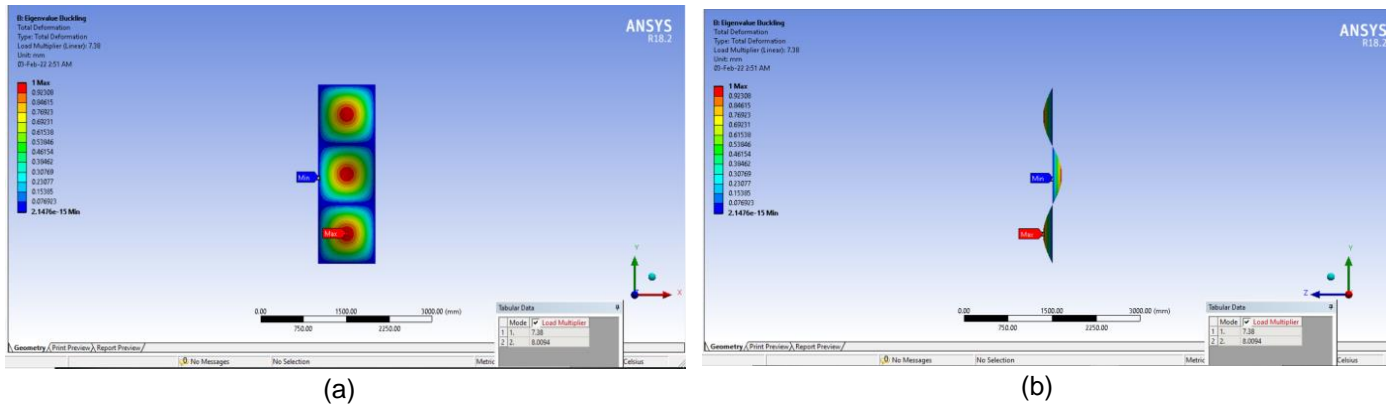


Figure 7. Eigen Value Buckling simulation results concerning optimized parameter wt. % of fibers as input: (a) Front view; (b) Side view.

CONCLUSION

Epoxy polymer composite, with sugarcane fiber, fly ash, and CNT as reinforcements, is fabricated to investigate its critical buckling load by varying the wt. % of the reinforcements. The 20 distinct samples, prepared by varying the weight percentages of the fiber reinforcements for each combination, are used for evaluation by implementing the Central Composite Design present in the Response Surface Methodology on Minitab. The Eigen Value Buckling standalone approach is used in the ANSYS18 software to simulate the combinations with varied wt. % of the reinforcements. Following the computational simulations of Eigenvalue buckling, statistical analysis is carried out on Minitab for obtaining a regression equation which is used to validate the critical buckling loads obtained computationally. The surface plots procured depict the influence of individual wt. % of reinforcements on critical buckling load. The optimized parametric results obtained at the end of the study represented the maximum critical buckling load which could be achieved with a combination of the wt. % of reinforcements accordingly. Based on the study conducted, the following conclusions are deduced.

- The regression equation shows that the critical buckling load tends to respond negatively to the weight percentages of the sugarcane and fly-ash and up to 0.75 wt. % of CNT, the critical buckling load increases and then decreases.
- Meanwhile, a minimal wt. % of CNT with either fly ash or sugarcane fiber tends to result in a minimal critical buckling load.
- A moderate wt. % of CNT as filler along with a significantly higher wt. % of sugarcane and fly ash offers comparatively higher critical buckling load.
- Error percentages are calculated between the computational simulation results and regression equation results to prove the compliance between both the results.
- A maximum critical buckling load of 80.80 N is thus obtained at 2 wt. % of sugarcane fiber, 0.75 wt. % of CNT and 2 wt. % of fly ash respectively.

Funding: This research received no external funding.

Conflicts of Interest: The authors declare no conflict of interest.

REFERENCES

1. Rhodes J. Some observations on the post-buckling behavior of thin plates and thin-walled members. *Thin-walled Struct.* 2003 Feb 1;41(2-3):207-26.
2. May-Pat A, Valadez-González A, Herrera-Franco PJ. Effect of fiber surface treatments on the essential work of fracture of HDPE-continuous henequen fiber-reinforced composites. *Polym. Test.* 2013 Sep 1;32(6):1114-22.
3. Philippou JL, Karastergiou SP. Lignocellulosic materials from annual plants and agricultural residues as raw materials for composite building materials. In *Proceedings of International Conference Forest Research: A Challenge for an Integrated European Approach*, Thessaloniki, Greece 2001 Aug 27 (Vol. 2, pp. 817-821).
4. Gutmann RJ. Advanced silicon IC interconnect technology and design: present trends and RF wireless implications. *IEEE Trans. Microw. Theory Tech.* 1999, 47(6):667-674.

5. Awaya N, Inokawa H, Yamamoto E, Okazaki Y, Miyake M, Arita Y, Kobayashi T. Evaluation of a copper metallization process and the electrical characteristics of copper-interconnected quarter-micron CMOS. *IEEE Trans. Electron Devices*. 1996, 43(8):1206-1212.
6. Allan A, Edenfeld D, Joyner WH, Kahng AB, Rodgers M, Zorian Y. 2001 technology roadmap for semiconductors. *Computer*. 2002 Aug 7;35(1):42-53.
7. Tan D, Tuncer E, Cao Y, Irwin P. Nanofiller dispersion in polymer dielectrics. *Mater. Sci. Appl*. 2013, 4(4): 6-15
8. Matuana LM, Stark NM. The use of wood fibers as reinforcements in composites. In *Biofiber reinforcements in composite materials 2015* Jan 1 (pp. 648-688). Woodhead Publishing.
9. Kumar GH, Babuvishwanath H, Purohit R, Sahu P, Rana RS. Investigations on mechanical properties of glass and sugarcane fiber polymer matrix composites. *Mater. Today: Proc*. 2017 Jan 1;4(4):5408-20.
10. Ticoalu A, Aravinthan T, Cardona F. A review of current development in natural fiber composites for structural and infrastructure applications. In *Proceedings of the southern region engineering conference (SREC 2010) 2010* (pp. 113-117). Engineers Australia.
11. Faruk O, Bledzki AK, Fink HP, Sain M. Biocomposites reinforced with natural fibers: 2000–2010. *Prog. Polym. Sci*. 2012, 1;37(11):1552-1596.
12. Arrakhiz FZ, El Achaby M, Malha M, Bensalah MO, Fassi-Fehri O, Bouhfid R, et al. Mechanical and thermal properties of natural fibers reinforced polymer composites: Doum/low density polyethylene. *Mater. Des*. 2013, 1; 43:200-205.
13. Di Bella G, Fiore V, Galtieri G, Borsellino C, Valenza A. Effects of natural fibres reinforcement in lime plasters (kenaf and sisal vs. Polypropylene). *Constr Build Mater*. 2014, 15;58:159-165.
14. Mohammed L, Ansari MN, Pua G, Jawaid M, Islam MS. A review on natural fiber reinforced polymer composite and its applications. *Int. J. Polym. Sci*. 2015, 1;2015.
15. Hajjiha H, Sain M. The use of sugarcane bagasse fibres as reinforcements in composites. In *Biofiber reinforcements in composite materials 2015* Jan 1 (pp. 525-549). Woodhead Publishing.
16. Huang Z, Wang N, Zhang Y, Hu H, Luo Y. Effect of mechanical activation pretreatment on the properties of sugarcane bagasse/poly (vinyl chloride) composites. *Compos Part A Appl. Sci Manuf*. 2012, 1;43(1):114-20.
17. Verma D, Gope PC, Maheshwari MK, Sharma RK. Bagasse fiber composites-A review. *J. Mater. Environ. Sci*. 2012;3(6):1079-92.
18. Vazquez A, Dominguez VA, Kenny JM. Bagasse fiber-polypropylene based composites. *J. Thermoplast. Compos. Mater*. 1999, 12(6):477-97.
19. Gopalan V, Suthenthiraveerappa V, David JS, Subramanian J, Annamalai AR, Jen CP. Experimental and Numerical Analyses on the Buckling Characteristics of Woven Flax/Epoxy Laminated Composite Plate under Axial Compression. *Polym*. 2021, 13(7):995.
20. Singla M, Chawla V. Mechanical properties of epoxy resin–fly ash composite. *J. Miner. Mater. Charac. Eng*. 2010, 20;9(3):199-210.
21. Sim J, Kang Y, Kim BJ, Park YH, Lee YC. Preparation of fly ash/epoxy composites and its effects on mechanical properties. *Polym*. 2020, 12(1):79.
22. Harris PJ. Carbon nanotube composites. *Int. mater. rev*. 2004, 1;49(1):31-43.
23. Gojny FH, Nastalczyk J, Roslaniec Z, Schulte K. Surface modified multi-walled carbon nanotubes in CNT/epoxy-composites. *Chem. Phys. Lett*. 2003, 21;370(5-6):820-4.
24. Keidar M, Levchenko I, Arbel T, Alexander M, Waas AM, Ostrikov K. Increasing the length of single-wall carbon nanotubes in a magnetically enhanced arc discharge. *Appl. Phys. Lett*. 2008, 28;92(4):043129.
25. Kim P, Shi L, Majumdar A, McEuen PL. Thermal transport measurements of individual multiwalled nanotubes. *Phys. Rev. Lett*. 2001, 31;87(21):215502.
26. Dai H, Rinzler AG, Nikolaev P, Thess A, Colbert DT, Smalley RE. Single-wall nanotubes produced by metal-catalyzed disproportionation of carbon monoxide. *Chem. Phys. Lett*. 1996, 27;260(3-4):471-5.
27. Yao Z, Kane CL, Dekker C. High-field electrical transport in single-wall carbon nanotubes. *Phys. Rev. Lett*. 2000, 27;84(13):2941.
28. Falvo MR, Clary GJ, Taylor R2, Chi V, Brooks FP, Washburn S, Superfine R. Bending and buckling of carbon nanotubes under large strain. *Nature*. 1997 Oct;389(6651):582-4.
29. Ahmadzai MD. Molecular Dynamics Research of a Carbon Nanotube-buckyball Enabled Energy Attraction System. *Int. J. Appl. Phys*. 2021, 28;9(2):125-138.
30. Lau AK, Hui D. The revolutionary creation of new advanced materials—carbon nanotube composites. *Compos. B. Eng*. 2002, 1;33(4):263-77.

31. Yao T, Fujikubo M. Buckling/Plastic Collapse Behavior and Strength of Rectangular Plate Subjected to Uni-Axial Thrust. *Buckling and Ultimate Strength of Ship and Ship-Like Floating Structures*, Butterworth-Heinemann, <https://doi.org/10.1016/C2015-0-00731-6>, 2016.
32. Mutu HB, Aslan Z. Experimental investigation of buckling behavior of E-glass/epoxy laminated composite materials with multi-walled carbon nanotube under uniaxial compression load. *J. Compos. Mater.* 2022, 56 (16): 2573-2584 <https://doi.org/10.1177/00219983221098795>, 2022.



© 2023 by the authors. Submitted for possible open access publication under the terms and conditions of the Creative Commons Attribution (CC BY NC) license (<https://creativecommons.org/licenses/by-nc/4.0/>).